KNOWING THE LIMITS OF A TREND: EXAMINING THE ONSET OF ASYMPTOTIC STABLE FRACTURE BEHAVIOUR IN MODE II FATIGUE DELAMINATION GROWTH

C. D. Rans[a,b*], J. Atkinson[b], C. Li[c]

[a]*Delft University of Technology, Department of Aerospace Structures and Materials, Delft, the Netherlands*
[b]*Carleton University, Department of Mechanical & Aerospace Engineering, Ottawa, Canada*
[c]*Institute for Aerospace Research, National Research Council of Canada, Ottawa, Canada*
**C.D.Rans@tudelft.nl*

Keywords: Mode II; fatigue; delamination growth, asymptotic behaviour.

Abstract
This study is motivated by the possibility that experimental data sets, particularly those obtained at high R-ratios, may unknowingly contain data points within the asymptotic stable fracture region that influence its perceived log-linear behaviour and the fit of various log-linear delamination growth models. Results from the experimental investigation indicate that the asymptotic stable fracture region can extend to G_{IImax} values as low as $0.7G_{IIc}$.

1. Introduction

It is generally accepted that fatigue delamination growth, analogous to metal fatigue crack growth, exhibits a sigmoidal behaviour when plotted against strain energy release rate on a log-log scale as illustrated in Figure 1. Numerous models for predicting growth focus on the log-linear region of the curve, also commonly known as the Paris region based on the early work of Paris et al. [1,2]. These models take a general form of the power law:

$$\frac{da}{dN} = C\left[f\left(G\right)\right]^n \tag{1}$$

Where da/dN is the delamination growth rate, *C* and *n* are empirical constants, assumed to be material constants, and *f(G)* is a formulation of the strain energy release rate. Common formulations include G_{max} and ΔG as discussed in [3].

Identification of the onset of each asymptotic region is important for the characterization and understanding of fatigue delamination behaviour. A relevant case study to illustrate this point is the study of R-ratio effects on fatigue delamination growth behaviour. In order to quantify the influence of R-ratio, fatigue delamination growth curves similar to that illustrated in Figure 1 are experimentally determined for constant R-ratios. Several curves are generated for different R-ratios and compared. When testing higher R-ratios, higher maximum fatigue loads are required to achieve comparable fatigue amplitudes as tested for lower R-ratios. In other words, G_{max} is necessarily increased to achieve a comparable ΔG. Thus, the threshold asymptote dependent on ΔG and the static failure asymptote dependent on G_{max} will move

closer to each other, narrowing the log-linear region of Figure 1, as the R-ratio is increased. As this narrowing effect increases, there is a risk that data points obtained from experiments that appear to maintain the log-linear trend when plotted actually lie within the asymptotic regions of the delamination growth curve.

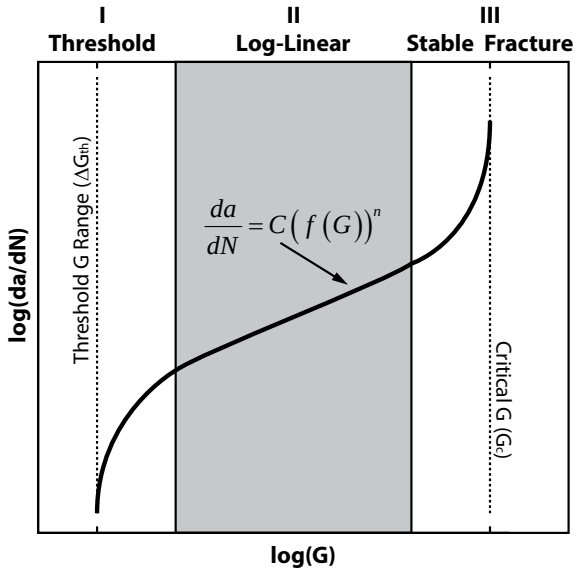

Figure 1. Sigmoidal behaviour of fatigue delamination growth vs strain energy release rate.

The possibility of the above case occurring can be illustrated with a data set from the literature plotted in Figure 2 [4]. In sub figure a, the data is plotted against G_{IImax} and appears to exhibit the expected log-linear behaviour. Plotting against the cyclic strain energy release rate range, $(\Delta\sqrt{G_{II}})^2$, proposed in [5], the data collapse to a common trend with the exception of a few data points indicated by **A** (see Figure 2). These data points correspond to test results where $G_{IImax} > 0.7G_{IIc}$. The remainder of this paper provides an overview of an experimental investigation into the possibility that these data points may lay within the asymptotic stable fracture region of the delamination growth behaviour curve.

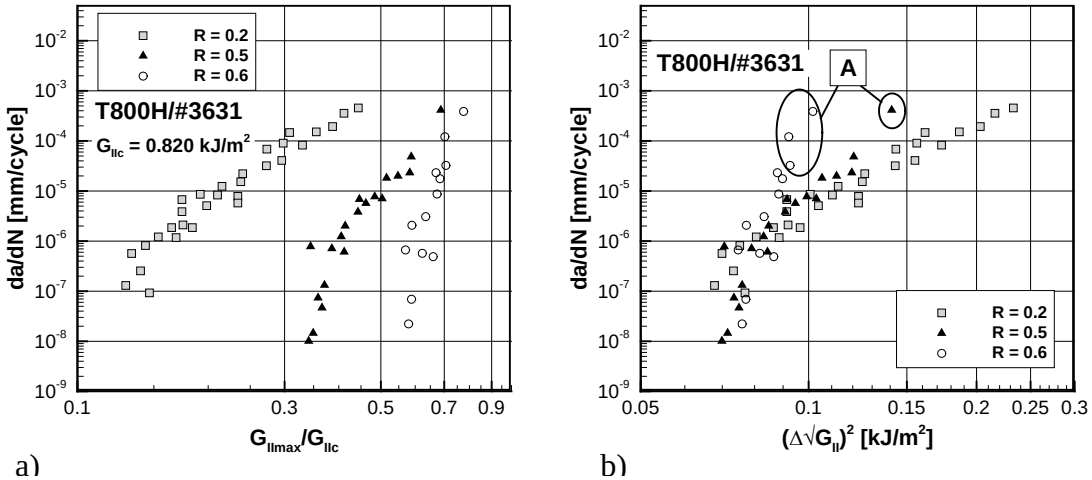

Figure 2. Experimental fatigue delamination growth data for IM7/8552 [4]; label A indicates data points where $G_{IImax} > 0.7G_{IIc}$.

2. Experimental Work

An experimental study was carried out in order to investigate the onset of an asymptote (denoted as the stable fracture region) in the Pairs-like behavior of Mode II fatigue delamination growth in composite.

Fatigue delamination growth tests were carried out with the so-called central cut-ply specimen used in previous studies of Mode II fatigue delamination growth in composite materials [6–9]. A similar specimen configuration, with a discontinuous metal layer, has also been used extensively to study Mode II fatigue delamination growth in hybrid Fibre Metal Laminate materials [10–16]. The test specimen consists of a series of discontinuous (or cut) plies laminated between continuous plies in a symmetric layup. The specimen geometry, including nominal dimensions used in this study, is illustrated in Figure 3. Specimens were fabricated from unidirectional M30SC/DT120 carbon epoxy prepreg material. Properties of the prepreg are given in Table 1.

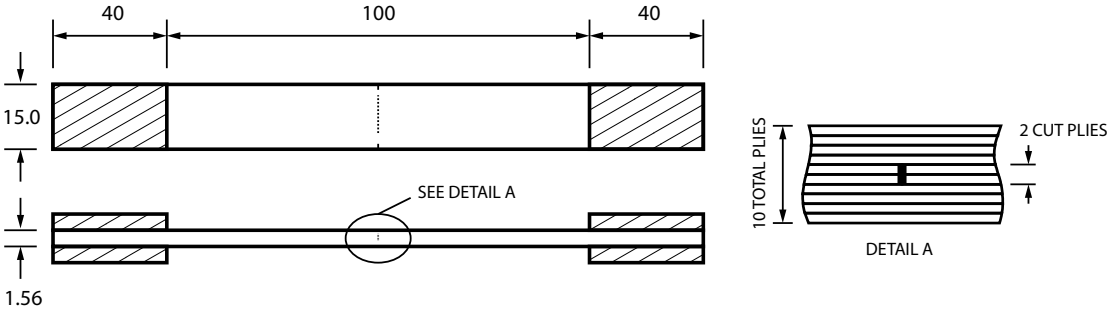

Figure 3. Details of the cut-ply specimen.

Fabrication of the specimens began with the production of four 160 mm x 300 mm rectangular carbon/epoxy laminates containing the central cut plies. These panels were cured at a temperature of 120°C and a pressure of 6 bars. Aluminum tabs were secondary-bonded to the rectangular laminates after curing. Specimens with a nominal width of 15 mm were cut from the rectangular panels using a lubricated diamond blade saw. A shorter specimen containing no cut plies was also cut from each panel and used to measure the Young's modulus of the material using a clip extensometer, which was found to be slightly below the manufacturer's quoted value (see Table 1).

Property	Manufacturer's Data	Measured Values
E_{11} [GPa]	155	145 ± 2.5
E_{22} [GPa]	7.8	-
G_{12} [GPa]	5.5	-
ν_{12}	0.27	-
G_{IIc} [kJ/m^2]	-	1.50 ± 0.05*

* Calculated using the measured Young's modulus

Table 1. Mechanical properties for unidirectional M30SC/DT120 prepreg.

The specimen geometry initiates four delaminations from the discontinuity in the laminate producing planar delaminations along the two interfaces between the continuous and discontinuous plies. A pure mode II shear field is applied to the delamination fronts through a far field tensile force, *P*, applied to the ends of the specimen. An expression for the strain energy release rate associated with each of the four delamination fronts was determined by Allegri et al. [8] and is summarized below:

$$G_{II} = \frac{P^2}{4B^2Et}\left(\frac{\chi}{1-\chi}\right) \tag{1}$$

where χ denotes the ratio of the number of cut plies to the total number of plies in the specimen, *B* and *t* are the specimen width and thickness respectively, and *E* is the Young's modulus of the material.

Table 2 defines the test space and number of specimens for the fatigue test program. The test space focused on the G_{IImax}/G_{IIc} range of 0.7 – 0.9 in order to identify the presence of a static failure asymptote in the delamination growth behaviour. A single specimen was used for each instance in the test matrix to avoid potential influences of variable amplitude loading on a specimen and to maximize the amount of delamination growth present for each calculation of growth rate. Delamination growth rates were determined by monitoring the change in peak strain readings obtained over the duration of the test with an MTS 634.12E-24 clip extensometer. As the strain energy release rate for the specimen is independent of delamination length (see equation (1)), the change in peak strain can be directly related to the delamination growth rate by the following equation:

$$\frac{da}{dN} = \frac{1-\chi}{\chi}\left(\frac{EBtL_{gauge}}{2P}\right)\frac{d\varepsilon^*}{dN} \tag{2}$$

Further details on the development of this equation can be found in journal paper by the present authors [17].

R	***G_{IImax}/G_{IIc}***								
	0.3	**0.4**	**0.5**	**0.6**	**0.7**	**0.75**	**0.8**	**0.85**	**0.9**
0.1	3	2	3	3	3	3	3	3	2
0.3	3	2	3	3	3	3	3	3	2
0.5	-	-	3	3	5	2	3	3	3

Table 2. Fatigue test matrix indicating the number of tests performed at each condition.

Fatigue tests were carried out on an MTS 810 servohydraulic test frame containing hydraulic wedge grips and a 100 kN load cell (model MTS 661.20E-03). The maximum and minimum forces for each test were calculated using equation (1), the measured specimen geometry, and the measured G_{IIc} value from Table 1. Tests were performed at frequencies varying between 1 – 5 Hz, where lower frequencies were primarily used for tests at G_{IImax}/Gc = 0.85 – 0.9 to increase the duration of the test, enabling visual inspections.

3. Results and Discussion

Delamination growth results from the test program are summarized in Figure 4. Delamination growth rates and strain energy release rates were calculated using equations (2) and (1)

respectively. Uncertainty due to measurement error is indicated by horizontal error bars for the strain energy release rate and by scatter in the various data points for delamination growth rate. Details of the error quantification can be found in [17]. Each data point represents the results from one test specimen according to the test matrix in Table 2.

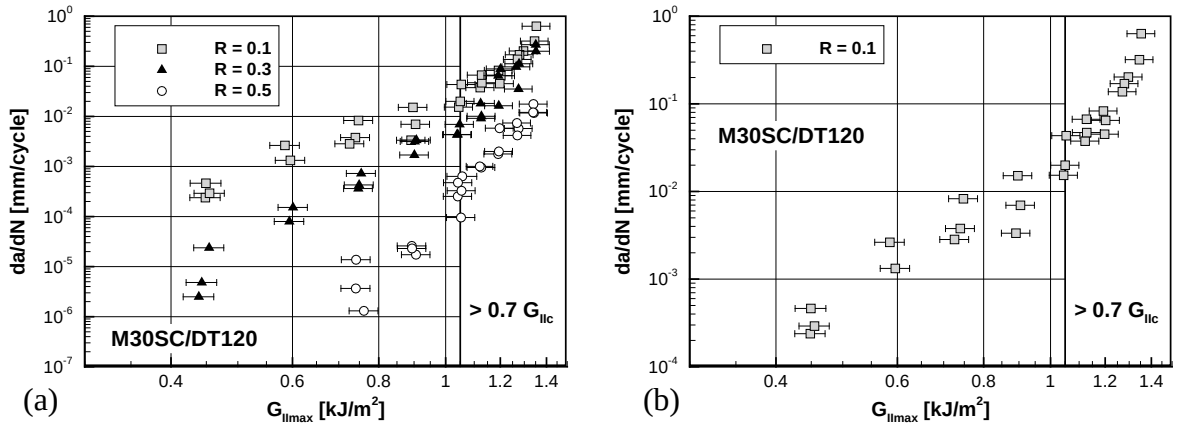

Figure 4. Experimental fatigue delamination growth results for MS30SC/DT120 (a) for all tests; rescaled to visualize non-linear behaviour on a log-log scale for (b) R = 0.1.

The delamination growth data in Figure 4a exhibits a non-linear behaviour on a log-log scale. To improve visualisation of this, the data set for R = 0.1 has been rescaled and plotted in Figure 4b. From this figure, the delamination growth data follows the typical linear log-log scale trend for G_{IImax} below approximately $0.7G_{IImax}$. Above this limit, the observed delamination growth rates rapidly increase, deviating from the previous linear trend, consistent with expectations for an asymptotic behaviour. This trend is clearly observed for the R = 0.1 and 0.3 data sets, however, it is difficult to ascertain for R = 0.5 due to the limited number of data points below the $0.7G_{IImax}$ limit and the large gradient in delamination growth behaviour below this limit.

It should be noted that there is no theoretical basis for the $0.7G_{IIc}$ limit discussed in this study. It is an observed limit consistent with the data from this study and the data from the literature given in Figure 2. Its value, however, is plausible in relation to the onset of a stable fracture mechanism. As discussed in [5], the strain energy release rate, G, is proportional to the square of the stress intensity factor, K, (or square of the applied stress). This is also evident from the proportionality between G_{II} and P^2 in equation (1). Thus, the limit $0.7G_{IIc}$ is equivalent to $0.84K_{IIc}$ or $0.84P_c$, where $0.84 = \sqrt{0.7}$. Given the local discontinuities in a composite laminate, it is plausible that localized unstable static fracture could occur this close to the fracture toughness of the material, resulting in accelerated delamination growth and the onset of the asymptotic stable fracture region.

This proportionality between G and K^2 also has implications on the definition of a cyclical strain energy release rate range. The cyclical stress intensity factor range, ΔK, typically used to characterize fatigue crack growth in metals, is a measure of the cyclic amplitude of the stress state ahead of a crack tip. It is dependent on the amplitude of this cyclic stress but independent of the mean stress, or in other words, dependent on the cyclic nature of the stress cycle but independent of its monotonic nature. The cyclic strain energy release rate, ΔG, often used as an analogy for ΔK in delamination growth does not have this same behaviour due to the above proportionality. From this proportionality, it follows that:

$$\Delta G \propto K_{\max}^2 - K_{\min}^2 = 2\left(\Delta K\right) K_{mean} \tag{3}$$

Thus, ΔG is dependent on the cyclic nature and mean (or monotonic) nature of the fatigue stress state. A more accurate analogy with ΔK would be to define the cyclical strain energy release rate range as $(\Delta\sqrt{G})^2$, as is discussed in [5]. This discussion is not meant to discredit the potential use of ΔG as a similitude parameter for characterizing delamination growth, but draw attention to its meaning, and the implication of its use. The authors, however, promote the use of the parameters $(\Delta\sqrt{G})^2$ and G_{max} as similitude parameters to characterize, respectively, the cyclic and monotonic nature of delamination growth independently.

Figure 5 shows the delamination growth data from this study plotted as a function of $(\Delta\sqrt{G_{II}})^2$, with all data points above the $0.7G_{IIc}$ limit highlighted in white. Here, the deviation of the delamination growth from a linear trend on a log-log scale becomes more apparent. Furthermore, the underlying trend for all R-ratios appears to be the same when plotted against $(\Delta\sqrt{G_{II}})^2$, indicating an absence of mean stress, or monotonic, effects on the delamination growth behaviour. This observation is consistent with previous observations discussed at the beginning of this paper and in [5].

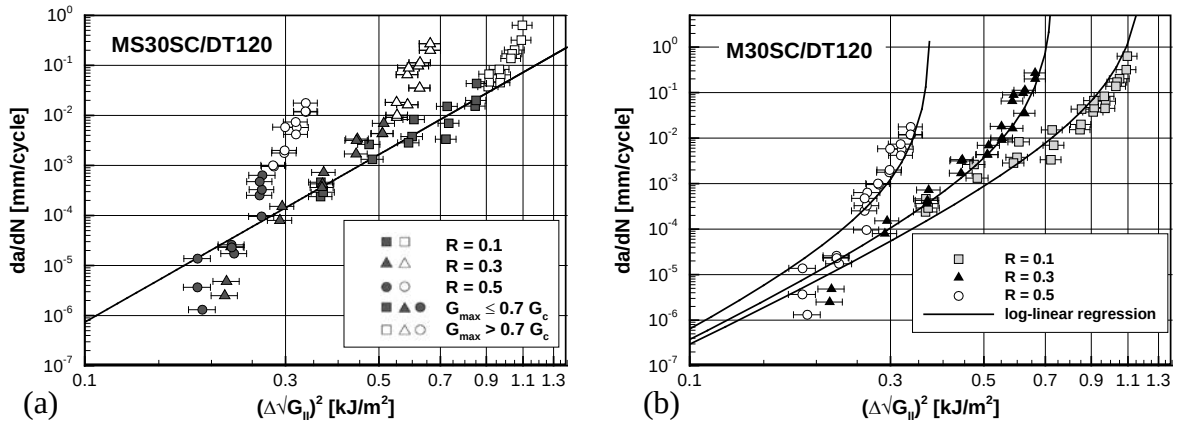

Figure 5. Fatigue delamination growth data plotted as a function of $(\Delta\sqrt{G_{II}})^2$ with (a) log-linear fit of data below identified onset and (b) Forman-like fit of data.

Above the $0.7G_{IIc}$ limit, the delamination growth behaviour does not converge to a single trend when plotted against $(\Delta\sqrt{G_{II}})^2$ (Figure 5) or G_{IImax} (Figure 4). This suggests that both cyclic and monotonic fracture mechanisms are present in this region. Indeed, it is logical that the introduction of local static fracture into the fracture process as G_{IIc} is approached would not completely remove the cyclic fracture mechanism.

To further illustrate the presence of the asymptote in the delamination growth data, a Forman-like relation was fitted to the data. The classical Forman equation takes the form of [18]:

$$\frac{da}{dN} = \frac{C\left(\Delta K\right)^b}{\left(1-R\right)\left(K_c - K_{\max}\right)} \tag{4}$$

where the factor of $(1 - R)$ in the denominator accounted for R-ratio effects and the factor $(K_c - K_{max})$ introduced the asymptotic behaviour in the stable fracture region. C and b are material dependent parameters.

In order to apply this equation to mode II delamination growth data in this study, the stress intensity factor values ($K_c - K_{max}$) and ΔK are substituted with $(\sqrt{G_{IIc}} - \sqrt{G_{IImax}})^2$ and $(\Delta\sqrt{G_{II}})^2$ respectively. Additionally, the term (1 – R) is dropped due to the absence of R-ratio effects for mode II delamination as discussed in [10] and as demonstrated for this data set in Figure 5a. The resulting modified Forman relation is thus given by:

$$\frac{da}{dN} = \frac{C\left(\Delta\sqrt{G_{II}}\right)^{2b}}{\left(\sqrt{G_{IIc}} - \sqrt{G_{II\,max}}\right)^2} \tag{5}$$

where the material dependent parameter *C* and *b* are different than those in equation (4).

Results from the regression of the data from this study using equation (5) are plotted in Figure 5b. The good agreement with the fit to the data further supports that an asymptotic behaviour is observed in the test results. Furthermore, the fit appears to support the identified $0.7G_{IIc}$ limit for onset observed in the tests. However, it should be noted that there is no physical basis within the Forman model for predicting this onset.

4. Conclusions

A series of fatigue tests have been performed to investigate the onset of the asymptotic stable fracture region in the Mode II fatigue delamination growth behaviour of a unidirectional carbon/epoxy material. Based upon the results of these tests, the following conclusions can be made:

- An asymptote in the delamination growth rate vs. maximum strain energy release rate behaviour of the material system under investigation was observed. This asymptote was most evident in the data sets obtained at fatigue stress ratios of 0.1 and 0.3.

- The onset of the asymptotic region appears to occur at approximately $0.7G_{IIc}$. Based on the strain energy release rate being proportional to the square of the stress intensity factor, this correlates with $0.84K_{IIc}$. This represents a plausible value for the onset of localized stable static delamination growth under fatigue loading given the local discontinuities within a composite laminate.

- Mode II fatigue delamination growth behaviour below the observed asymptote shows a good correlation with $(\Delta\sqrt{G})^2$, consistent with previous findings of the authors [5] and consistent with other studies [4], [19] utilizing an analogous stress intensity factor description, ΔK.

References

[1] P. C. Paris, M. P. Gomez and W. E. Anderson. A rational analytic theory of fatigue. *The Trend in Engineering*, 13:9–14, 1961.

[2] P. C. Paris and F. Erdogan. A Critical Analysis of Crack Propagation Laws. *Journal of Basic Engineering*, 85(4):528-533, 1963.

[3] J. A. Pascoe, R. C. Alderliesten and R. Benedictus. Methods for the prediction of fatigue delamination growth in composites and adhesive bonds – A critical review. *Engineering Fracture Mechanics*, 112–113:72–96, 2013.

[4] K. Tanaka and H. Tanaka. Stress-ratio effect on mode II propagation of interlaminar fatigue cracks in graphite/epoxy composites. In Armanios E. A., editor, *Composite Materials: Fatigue and Fracture (Sixth Volume)*, pages 126-142, ASTM International, 1997.

[5] C. D. Rans, R. C. Alderliesten and R. Benedictus. Misinterpreting the results: How similitude can improve our understanding of fatigue delamination growth. *Composites Science and Technology*, 71(2):230–238, 2011.

[6] L. F. Kawashita, M. I. Jones, R. S. Trask, S. R. Hallett and M. R. Wisnom. Static and fatigue delamination from discontinuous plies - Experimental and numerical investigations. In *ICCM International Conferences on Composite Materials*, 2009.

[7] M. R. Wisnom, M. I. Jones and W. Cui. Delamination in composites with terminating internal plies under tension fatigue loading. In Martin R. H., editor, *Composite Materials: Fatigue and Fracture (Fith Volume)*, pages 486-508, ASTM International, 1995.

[8] G. Allegri, M. I. Jones, M. R. Wisnom and S. R. Hallett. A new semi-empirical model for stress ratio effect on mode II fatigue delamination growth. *Composites Part A: Applied Science and Manufacturing*, 42(7):733–740, 2011.

[9] M. R. Wisnom and M. Jones. An Experimental and Analytical Study of Delamination of Unidirectional Specimens with Cut Central Plies. *Journal of Reinforced Plastics and Composites*, 13(8):722–739, 1994.

[10] C. D. Rans, R. C. Alderliesten and R. Benedictus. Predicting the influence of temperature on fatigue crack propagation in Fibre Metal Laminates. *Engineering Fracture Mechanics*, 78(10):2193–2201, 2011.

[11] R. Marissen. *Fatigue crack growth in ARALL: A hybrid aluminium-aramid composite material*. PhD dissertation, Delft Univerity of Technology, 1988.

[12] C. T. Lin and P. W. Kao. Fatigue delamination growth in carbon fibre-reinforced aluminium laminates. *Composites Part A: Applied Science and Manufacturing*, 27(1):9–15, 1996.

[13] S. U. Khan, R. C. Alderliesten and R. Benedictus. Delamination growth in Fibre Metal Laminates under variable amplitude loading. *Composites Science and Technology*, 69(15–16):2604–2615, 2009.

[14] D. A. Burianek and S. M. Spearing. Delamination growth from face sheet seams in cross-ply titanium/graphite hybrid laminates. *Composites Science and Technology*, 61(2):261–269, 2001.

[15] R. C. Alderliesten, J. Schijve and S. van der Zwaag. Application of the energy release rate approach for delamination growth in Glare. *Engineering Fracture Mechanics*, 73(6):697–709, 2006.

[16] R. C. Alderliesten. *Fatigue Crack Propagation and Delamination Growth in GLARE*. PhD dissertation, Delft University of Technology, 2005.